Modeling and Control of Casterboard Robot

Kazuki KINUGASA * **Masato ISHIKAWA** *
Yasuhiro SUGIMOTO * **Koichi OSUKA** *

* *Department of Mechanical Engineering, Graduate School of Engineering, Osaka University, Japan, (e-mail: ishikawa@mech.eng.osaka-u.ac.jp)*

Abstract: In this paper, we propose a robotic model of a casterboard, which is a commercial variants of skateboards with twistable footplates and passive inclined caster wheels. We then derive its mathematical model in the form of nonlinear state equation; this system is of much interest from both mechanical and control points of view as a new challenging example of nonholonomic mechanics. Based on the observation on preceding works concerning locomotion control for nonholonomic systems, we propose a locomotion control method with sinusoidal periodic control to realize forwarding and turning locomotion. The proposed idea is examined by simulations and physical experiments using the prototype robot developed by the authors. Moreover, we also examine the influences on the driving of the robot of parameter in the sinusoidal reference signals.

1. INTRODUCTION

In this paper, we propose a robotic model of a *casterboard*, which is a commercial variants of skateboards with twistable footplates and passive inclined caster wheels (as shown in Fig. 1). The casterboard has an peculiar body structure that the board itself is divided into two parts, the front and the rear wheels can be steered separately to each other. By appropriate combinatory actions of one's waist and feet, a human rider can drive the casterboard without kicking the ground directory. This seems a quite challenging and fascinating example from viewpoints of both control theory and robotics. Our purpose is to clarify the principle of casterboard locomotion through control experiment of its prototype robot.

As closely related works to the current problem, there have been a series of studies on *snakeboard* system conducted by Ostrowski et al. (see Ostrowski et al. [1995, 1997], Ostrowski and Burdick [1998], McIsaac and Ostrowski [2003] and the references therein). The snakeboard is also a variant of skateboards having twistable casters at the both ends, and undulatory propulsion without kicking the ground is possible likewise in the casterboards. Ostrowski et. al. derived a mathematical model of the snakeboard based on nonholonomic mechanics, in the form of nonlinear state equation composed of (i) geometric equation, (ii) generalized momentum equation and (iii) reduced equation (see Murray et al. [1994], Bloch [2003]). A notable feature here is the presense of (ii) and coupled influences between (i) and (ii). The authors also worked on point-to-point feedback control of the snakeboard considering repetitive stability of its generalized momentum (see Kiyasu and Ishikawa [2006]).

Modeling and control of the casterboard appears to be harder than the snakeboard, in that it has complicated footplate-caster mechanism and its dynamics is inherently three-dimensional. Shammas and Choset proposed *variable inertia snakeboard* which is a general framework including the snakeboard as its special case, in that the inertia matrix depends on the configuration of the robot, and simulated forwarding locomotion of casterboard by controlling it in specific configurations (see Shammas and Choset [2006]). However they have not exploited various driving modes of casterboard which appear by changing parameters of inputs, and with experiments.

In this paper, we suggest a control approach for casterboard locomotion together with its dynamical model. Slightly from a different viewpoint compared to the previous work, we show that the casterboard can be controled with an approach similar to the aforementioned snakeboard at the cost of some simplifying assumptions. We then model the casterboard as an autonomous mobile robot with active weights, and propose a control approach for forwarding and turning locomotion based on sinusoidal reference signals. The proposed idea is examined by both simulations and experiments. Moreover, we also examine the influences on the driving of phase difference and frequency of sinusoidal reference signals by both simulations and experiments.

This paper is organized as follows. After brief review of snakeboard research in Section 2, we propose a robotic version of the casterboard and derive its mathematical model in Section 3. Control strategy is proposed and examined numerically and experimentally in Section 4. Influences of phase difference in the reference signals are examined in Section 5. Section 6 concludes the paper.

2. BACKGROUND: SNAKEBOARD ROBOT

In this section, we briefly review the relevant studies on snakeboard robots mainly conducted by Ostrowski et. al. (see Ostrowski and Burdick [1998]).

(a) Casterboard (b) Snakeboard

Fig. 1. Casterboard and Snakeboard

Snakeboard is a commercial variant of skateboard which has been somewhat popular in playground scene since mid-90's. It is composed of a main beam and two footplates with passive wheels at the both ends (front and rear) as shown in Fig. 2. Each footplate is connected to the main beam via a rotary joint about the vertical axis, so that the front wheels and the rear wheels can be steered using the rider's feet relative to the main beam. Basically, maneuvering principle of the snakeboard for a rider is a (skillful) combination of the following actions:

- to steer the footplates into the direction opposite to each other
- to exert yaw-torque around the body center by twisting one's waist

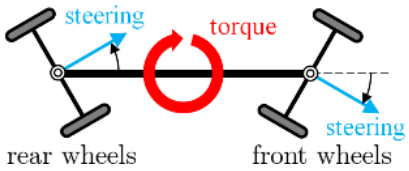

Fig. 2. Maneuvering basics of the snakeboard

Ostrowski et al. discussed a mathematical description of the snakeboard dynamics, and proposed an autonomous robot model of the snakeboard, i.e., a *snakeboard robot* (see Ostrowski et al. [1995]). It has a rotor which exerts torque to the snakeboard about the vertical axis passing through the body center, via an active joint Ψ as shown in Fig. 3. The model has been formulated as a nonholonomic dynamical system which has generalized momentum as a state (see Murray et al. [1994], Bloch [2003]). Moreover, inputs to the system for propulsion control have been derived based on the analysis of controllability with Lie brackets of vector fields in the state equation of the model. They also simplified the model by assuming that the front and the rear footplates are driven in symmetric way (with a common control parameter Φ), thus reduced the problem to a nonlinear system with two control inputs $\dot{\Phi}$ and $\ddot{\Psi}$.

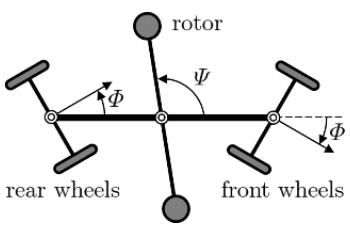

Fig. 3. Model of the snakeboard robot

According to these results, given that each wheels is in contact with the ground without slipping nor sliding sideways, forwarding locomotion and turning locomotion of the snakeboard robot are controllable by varying the rotational angle of the rotor Ψ and the steering angle of the wheels Φ periodically with a common frequency. Their success motivates us to challenge to other sort of "weired" dynamic boards.

3. CASTERBOARD ROBOT

In this section, we introduce the dynamics of casterboard and propose its robotic model.

3.1 Modeling

Fig. 4 illustrates a schematic side view of the casterboard (shown in Fig. 1). The casterboard consists of a front board and a rear board joined to each other via rotary joint about the horizontal (roll) axis. Each board is equipped with a passive caster inclined by a certain constant angle. Both boards can be twisted to each other about the roll-axis as the rider "presses" the boards by his/her feet. The casters also rotate about their incline axes. Therefore, when the rider *presses down* the boards to make them roll, each wheel is *pushed out* to the opposite direction, so as to minimize the potential energy as shown in Fig. 5. In short, the caster's yaw angle ψ is indirectly steered when one steers the board's roll angle ϕ.

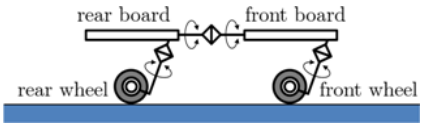

Fig. 4. Side view of the casterboard

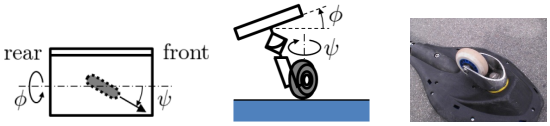

(a) Top view (b) Front view (c) Actual caster

Fig. 5. Relationship between the boards and the caster wheels

This leads us to explain the basic maneuvering principle for the casterboard, as shown in Fig. 6. Rolling both boards alternately, exerting force in the direction which each board is tilted toward (labeled as "force" in the figure) by each foot of the rider. This explanation is in rough accordance with the techniques performed by experienced riders. These actions of the feet generate torque around the vertical axis of the casterboard, with both wheels being steered in the opposite direction from each other, which result in forward movement of the casterboard.

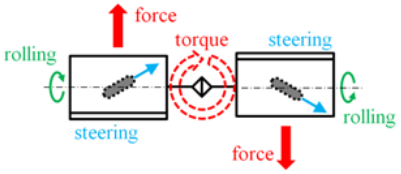

Fig. 6. Maneuvering basics of the casterboard

3.2 Casterboard "Robot"

Now we are ready to model the casterboard as an autonomous mobile robot (casterboard robot) using active mass drivers instead of a human rider. See Fig. 7 for the proposed robotic model of the casterboard. The robot is supposed to consist of two blocks, the front and the rear ones. Each block is equipped with a mass on its top side, connected by a rigid beam, where the center of the wheel is located just beneath the bottom end of the rigid beam. The front and the rear block are connected to each other by an *active* twistable joint, which we suppose to apply control inputs.

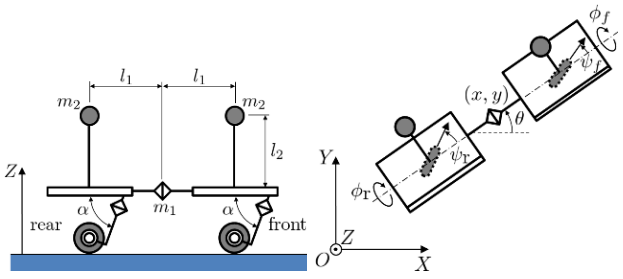

(a) Side view (b) Top view

Fig. 7. Model of the casterboard robot

3.3 Derivation of the state equation

Let us derive the state equation of the casterboard robot. In Fig. 3.2, (x, y) denotes the robot's position, i.e., the coordinates of the centeral joint on X-Y plane. θ is the attitude angle relative to the X-axis. ϕ_f, ϕ_r are roll angles of front and rear board, respectively. ψ_f, ψ_r are steering angles of front and rear wheel, respectively.

Here we dare to compromise on following assumptions to simplify the problem.

[Assumptions]

(1) Roll orientation of the robot is always *kept upright*.
(2) Roll angle of boards ϕ_i $(i = f, r)$ is very small, so we obtain the following approximate expressions:
$$\sin\phi_i \approx \phi_i, \quad \cos\phi_i \approx 1. \tag{1}$$
(3) In response to the change of roll angle of the board ϕ_i, yaw angle of the wheels ψ_i changes instantaneously due to their inclined configuration (Fig. 7). Namely, ϕ_i and ψ_i satisfy the following *holonomic* constraint:
$$\psi_i(t) = \tan^{-1}(\tan\alpha \sin\phi_i(t)). \tag{2}$$
Eq. (2) is derived from the configuration of each caster when the potential energy of the robot is minimum.

These assumptions may seem somewhat restrictive. However, at the cost of this compromise, we can reduce the problem to control problem for an almost *planar* mobile robot nevertheless the original system is three-dimensional. It would be clear in the rest of paper that essence of the casterboard locomotion still remains in this reduced planar model.

Now we introduce several physical parameters. m_1 denotes mass of the entire robot, m_2 denotes mass of a weight, l_1 is length from the center of the robot to one wheel, l_2 is length of the rigid beam (distance between the mass and the board), J denotes moment of inertia of the robot about the vertical axis. α is a constant that indicate incline angle of the caster axis relative to the vertical axis. The Lagrangian of the whole system is given by

$$\begin{aligned} L =& \frac{1}{2}m_1(\dot{x}^2+\dot{y}^2) + \frac{1}{2}J\dot{\theta}^2 \\ &+ \frac{1}{2}m_2\left[\left\{\frac{\mathrm{d}}{\mathrm{d}t}(x + l_1\cos\theta - l_2\phi_f\sin\theta)\right\}^2\right. \\ &\quad \left.+ \left\{\frac{\mathrm{d}}{\mathrm{d}t}(y + l_1\sin\theta + l_2\phi_f\cos\theta)\right\}^2\right] \\ &+ \frac{1}{2}m_2\left[\left\{\frac{\mathrm{d}}{\mathrm{d}t}(x - l_1\cos\theta - l_2\phi_r\sin\theta)\right\}^2\right. \\ &\quad \left.+ \left\{\frac{\mathrm{d}}{\mathrm{d}t}(y - l_1\sin\theta + l_2\phi_r\cos\theta)\right\}^2\right]. \end{aligned} \tag{3}$$

In Eq. (3), the first line denotes kinetic energy of the body except weights, the second and the third lines denote kinetic energy of the front weight, and the fourth and the fifth lines denote kinetic energy of the rear weight. Here, gravitational potential energy is not considered due to Eq. (1). Assuming all the wheels do not slide sideways, we obtain the following nonholonomic constraints:

$$\begin{cases} \dot{x}\sin(\theta+\psi_f) - \dot{y}\cos(\theta+\psi_f) - l_1\dot{\theta}\cos\psi_f = 0 \\ \dot{x}\sin(\theta+\psi_r) - \dot{y}\cos(\theta+\psi_r) + l_1\dot{\theta}\cos\psi_r = 0 \end{cases}. \tag{4}$$

Thanks to the assumptions mentioned above, the generalized coordinates of the system is composed of just $\boldsymbol{q} := [\boldsymbol{w}, \phi_f, \phi_r]^{\mathrm{T}}$, where $\boldsymbol{w} := [x, y, \theta]^{\mathrm{T}}$ indicates the *location* of the entire robot. First, the Lagrangian equation of motion with respect to ϕ_f, ϕ_r is described as follows.

$$\begin{cases} m_2 l_2^2\ddot{\phi}_f - m_2 l_2(\ddot{x}\sin\theta - \ddot{y}\cos\theta - l_1\ddot{\theta}) \\ \qquad - \left(\frac{1}{2}m_2 l_1 l_2\cos 2\theta - l_2^2\phi_f\right)\dot{\theta}^2 = \tau_f \\ m_2 l_2^2\ddot{\phi}_r - m_2 l_2(\ddot{x}\sin\theta - \ddot{y}\cos\theta + l_1\ddot{\theta}) \\ \qquad + \left(\frac{1}{2}m_2 l_1 l_2\cos 2\theta - l_2^2\phi_r\right)\dot{\theta}^2 = \tau_r \end{cases} \tag{5}$$

Here τ_f, τ_r are external torques applied as the actuator inputs. Following the standard manner of computed torque method, it is not difficult to consider $\boldsymbol{u} := [\ddot{\phi}_f, \ddot{\phi}_r]^{\mathrm{T}}$ as a virtual control input.

On the other hand, combining Eq. (2) and Eq. (4) gives us a kinematic constraint linear in $\dot{\boldsymbol{w}}$

$$D(\boldsymbol{q})\dot{\boldsymbol{w}} = 0,$$
$$D(\boldsymbol{q}) := \begin{bmatrix} \sin(\theta+\psi_f(\phi_f)) & -\cos(\theta+\psi_f(\phi_f)) & -l_1\cos\psi_f(\phi_f) \\ \sin(\theta+\psi_r(\phi_r)) & -\cos(\theta+\psi_r(\phi_r)) & l_1\cos\psi_r(\phi_r) \end{bmatrix} \tag{6}$$

Thus the Lagrangian equation of motion with respect to the location vector $\boldsymbol{w}$ under the constraint (6) is derived as in the following form, with the Lagrange multiplier $\boldsymbol{\lambda} = [\lambda_1, \lambda_2]^{\mathrm{T}}$ to indicate constraint forces:

$$M\ddot{\boldsymbol{w}} + W(\boldsymbol{q}) - E(\boldsymbol{q})\boldsymbol{u} - D(\boldsymbol{q})^T\boldsymbol{\lambda} = 0 \tag{7}$$

where $M(\boldsymbol{q}), W(\boldsymbol{q})$ and $E(\boldsymbol{q})$ are given by

$$M(\boldsymbol{q}) = \begin{bmatrix} m_1+2m_2 & 0 & M_{13} \\ 0 & m_1+2m_2 & M_{23} \\ M_{13} & M_{23} & M_{33} \end{bmatrix}$$
$$M_{13} = -m_2 l_2(\phi_f+\phi_r)\cos\theta$$
$$M_{23} = -m_2 l_2(\phi_f+\phi_r)\sin\theta$$
$$M_{33} = J + m_2\{2l_1^2 + l_1 l_2(\phi_f-\phi_r)\cos 2\theta + l_2^2(\phi_f^2+\phi_r^2)\}$$
$$W(\boldsymbol{q}) = \begin{bmatrix} W_1 \\ W_2 \\ W_3 \end{bmatrix}$$
$$W_1 = m_2 l_2\{(\phi_f+\phi_r)\sin\theta\cdot\dot{\theta} - 2(\dot{\phi}_f+\dot{\phi}_r)\cos\theta\}\dot{\theta} + c\dot{x}$$
$$W_2 = -m_2 l_2\{(\phi_f+\phi_r)\cos\theta\cdot\dot{\theta} - 2(\dot{\phi}_f+\dot{\phi}_r)\sin\theta\}\dot{\theta} + c\dot{y}$$
$$W_3 = m_2 l_2[l_1\{(\dot{\phi}_f-\dot{\phi}_r)\cos 2\theta - (\phi_f-\phi_r)\sin 2\theta\cdot\dot{\theta}\} + 2l_2(\phi_f\dot{\phi}_f+\phi_r\dot{\phi}_r)]\dot{\theta} + 2cl_1^2\dot{\theta}$$
$$E(\boldsymbol{q}) = \begin{bmatrix} m_2 l_2\sin\theta & m_2 l_2\sin\theta \\ -m_2 l_2\cos\theta & -m_2 l_2\cos\theta \\ -m_2 l_1 l_2 & m_2 l_1 l_2 \end{bmatrix}$$

Here, we assume that both wheels are subjected to viscosity resistance from ground along their moving direction. Above c is proportionality constant in the viscosity resistance.

Solving Eq. (7) using Eq. (6), $\boldsymbol{\lambda}$ is given by

$$\boldsymbol{\lambda} = (DM^{-1}D^{\mathrm{T}})^{-1}(-\dot{D}\dot{\boldsymbol{w}} + DM^{-1}W - DM^{-1}E\boldsymbol{u}). \tag{8}$$

Eliminating $\boldsymbol{\lambda}$ from Eq. (7) using Eq. (8), we have:

$$\ddot{\boldsymbol{w}} + Q\dot{D}\dot{\boldsymbol{w}} + PM^{-1}W - PM^{-1}E\boldsymbol{u} = 0 \tag{9}$$

where $Q(\boldsymbol{q})$ and $P(\boldsymbol{q})$ are given by

$$Q(\boldsymbol{q}) = M^{-1}D^{\mathrm{T}}(DM^{-1}D^{\mathrm{T}})^{-1}$$
$$P(\boldsymbol{q}) = I - QD$$

Here, I is an unit matrix. Therefore the state equation of the casterboard robot is described as follows.

$$\frac{\mathrm{d}}{\mathrm{d}t}\begin{bmatrix} \boldsymbol{w} \\ \dot{\boldsymbol{w}} \\ \phi_f \\ \phi_r \\ \dot{\phi}_f \\ \dot{\phi}_r \end{bmatrix} = \begin{bmatrix} \dot{\boldsymbol{w}} \\ -Q\dot{D}\dot{\boldsymbol{w}} - PM^{-1}W \\ \dot{\phi}_f \\ \dot{\phi}_r \\ 0 \\ 0 \end{bmatrix} + \begin{bmatrix} 0 & 0 \\ PM^{-1}E & \\ 0 & 0 \\ 0 & 0 \\ 1 & 0 \\ 0 & 1 \end{bmatrix}\boldsymbol{u} \tag{10}$$

Note again that D, W, E, Q and P are all matrix-valued nonlinear functions depend on the state variables.

4. LOCOMOTION CONTROL

In this section, we propose a control approach for the casterboard robot, whose validity is examined both by numerical simulations and physical experiments.

4.1 Control approach

Now we intend to control the roll angle ϕ_f, ϕ_r of the casterboard robot to track respectively the sinusoidal reference angle $\phi_f^{\mathrm{ref}}, \phi_r^{\mathrm{ref}}$ given as follows, so that the steering angle of each wheel and torque exerted on the body changes periodically with a common frequency:

$$\phi_f^{\mathrm{ref}}(t) = A\sin\omega t + B \tag{11}$$
$$\phi_r^{\mathrm{ref}}(t) = -\phi_f^{\mathrm{ref}}(t) \tag{12}$$

where A is the amplitude, B is the average of oscillation and ω denotes the angular frequency. B determines the direction (or turning radius) of locomotion : $B = 0$ corresponds to forwarding locomotion, while $B \neq 0$ corresponds to turning locomotion where $B > 0$ for counter-clockwise rotation and $B < 0$ for clockwise rotation.

As for the tracking control of ϕ_f, ϕ_r to the reference angle $\phi_f^{\mathrm{ref}}, \phi_r^{\mathrm{ref}}$, we simply adopt the following feedback PD-type control law:

$$\boldsymbol{u} = \begin{bmatrix} K_P(\phi_f^{\mathrm{ref}}-\phi_f) + K_D(\dot{\phi}_f^{\mathrm{ref}}-\dot{\phi}_f) + \ddot{\phi}_f^{\mathrm{ref}} \\ K_P(\phi_r^{\mathrm{ref}}-\phi_r) + K_D(\dot{\phi}_r^{\mathrm{ref}}-\dot{\phi}_r) + \ddot{\phi}_r^{\mathrm{ref}} \end{bmatrix} \tag{13}$$

where $\phi_f^{\mathrm{ref}}, \phi_r^{\mathrm{ref}}$ are the reference angles, K_P is the proportional gain and K_D is the derivative gain.

4.2 Simulation

In this subsection, the proposed approach is examined by several numerical simulations based on the state equation (10). Here, the values of the parameters A, B and T in the reference angles $\phi_f^{\mathrm{ref}}, \phi_r^{\mathrm{ref}}$ were given as follows.

- Forwarding locomotion :

$$A = \frac{\pi}{9}\ [\mathrm{rad}],\ B = 0\ [\mathrm{rad}],\ \omega = 6.4\ [\mathrm{rad/s}]$$

- Turning locomotion :

$$A = \frac{\pi}{18}\ [\mathrm{rad}],\ B = \frac{\pi}{18}\ [\mathrm{rad}],\ \omega = 11.4\ [\mathrm{rad/s}]$$

The value of each parameter in the state equation (10) was given as shown in Table 1. Here, for simplicity, let $J = \frac{m_1 l_1^2}{3}$ by putting the body a bar of uniform cross-section. The values of K_P and K_D were given so that ϕ_i follows ϕ_i^{ref} sufficiently. The other values in Table 1 were given so as to be the same as in the prototype shown in the following section. Incidentally, the initial location was $\boldsymbol{w}(0) = [0, 0, 0]^{\mathrm{T}}$.

Table 1. Physical parameters of the casterboard robot

l_1	length from the center of the body to a wheel	0.095 [m]
l_2	length of the inverted pendulum	0.115 [m]
m_1	mass of the body	1.29 [kg]
m_2	mass of a weight	0.29 [kg]
J	inertia of the body about the vertical axis	0.039 [kg·m^2]
α	incline angle of the caster axis	$\frac{7}{18}\pi$ [rad]
c	proportionality constant in viscosity resistance between wheels and ground	0.8 [N·s/m]

First, the simulation result of forwarding locomotion is shown in Fig. 8. As shown in the figures, the casterboard robot moves forward winding its way.

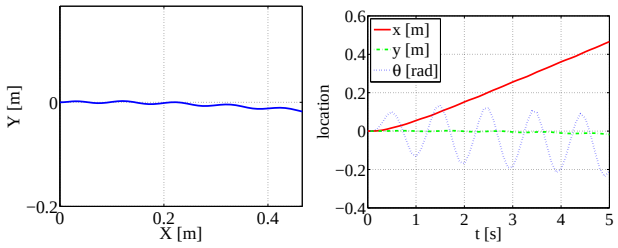

(a) X-Y trajectory (b) Robot's location

Fig. 8. Simulation of forwarding locomotion

Second, the simulation result of turning locomotion is shown in Fig. 9. As shown in the figures, the casterboard robot turns. Here, the turning radius is almost constant. Moreover, it was also confirmed that the model of the

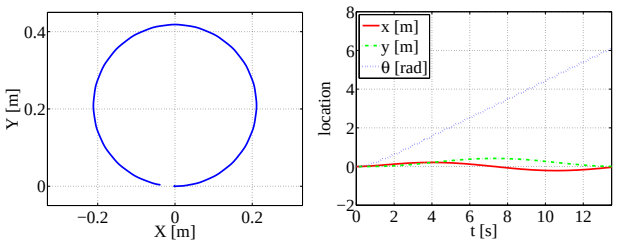

(a) X-Y trajectory (b) Robot's location

Fig. 9. Simulation of turning locomotion

casterboard robot was valid from the above results.

4.3 Experiment

We developed a prototype of microcomputer-controlled casterboard robot as shown in Fig. 10. This prototype has

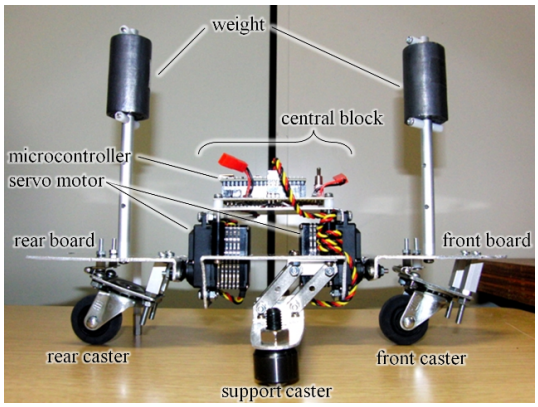

Fig. 10. Overview of the casterboard robot

the front and the rear boards (footplates), each of which is equipped with a weight and a caster. It also has the central block put between the both boards so as to control rolling of each board. The central block has two servomotor at the front and the rear side, connected to the front and the rear boards, respectively.

In addition, we attach a support caster consisting of two ball casters to the bottom of the central block, through a parallel link mechanism so that the casters are kept horizontal. As a result, the central block does not roll irrespective of its vertical motion. Therefore the roll angle of each board ϕ_i is given on the basis of the central block by each servomotor.

The proposed approach is examined by several experiments. We adopted the same reference signals to the servomotors $\phi_f^{\mathrm{ref}}(t), \phi_r^{\mathrm{ref}}(t)$ as in simulations mentioned above. Fig. 11 shows the experimental result of forwarding locomotion. The casterboard robot surely moves forward with a certain amount of winding, likewise in the simulation results.

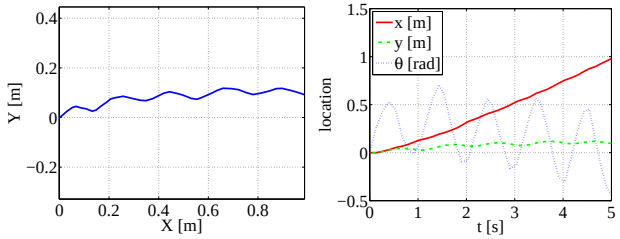

(a) X-Y trajectory (b) Robot's location

Fig. 11. Experiment of forwarding locomotion

Second, the experimental result of turning locomotion is shown in Fig. 12. The casterboard robot also exhibits

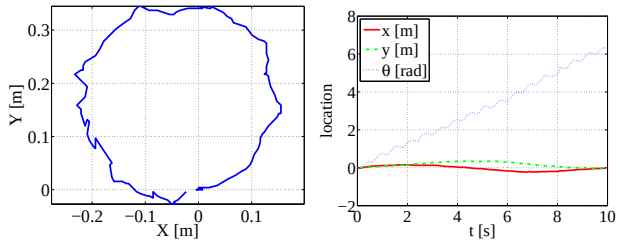

(a) X-Y trajectory (b) Robot's location

Fig. 12. Experiment of turning locomotion

counter-clockwise turning with almost constant radius, also likewise in the simulation results.

5. INFLUENCE OF PHASE DIFFERENCE

In the last section, we have been considering to drive roll angles of the both boards in *anti-phase manner*. Now we examine how the phase difference between ϕ_f^{ref} and ϕ_r^{ref} affects on the resulting locomotion.

5.1 Simulation

First, we examine the influence of phase difference of front and rear boards by numerical simulations based on the

state equation (10). The reference signals $\phi_f^{\mathrm{ref}}, \phi_r^{\mathrm{ref}}$ were given in the following forms:

$$\begin{cases} \phi_f^{\mathrm{ref}}(t) = A\sin\omega t \\ \phi_f^{\mathrm{ref}}(t) = A\sin(\omega t - \beta) \end{cases} \tag{14}$$

where A is the common amplitude, ω is the common angular frequency and β is the phase difference between the two signals. Now we fix $A = \pi/9$ [rad], $\omega = 6.4$ [rad/s], set the initial location as $\boldsymbol{w}(0) = [0, 0, 0]^{\mathrm{T}}$, and see what happens with various phase gaps $\beta = 0, \pi/2, \pi$ [rad].

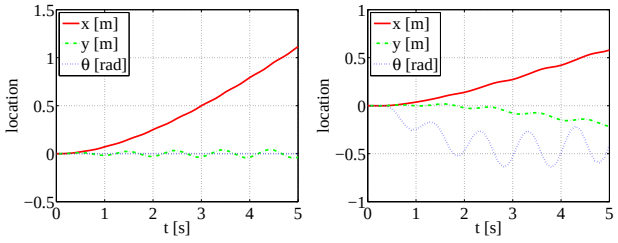

(a) $\beta = 0$ [rad] (b) $\beta = \pi/2$ [rad]

Fig. 13. Robot's location (simulation)

Fig. 13 shows the simulation results. Note we omit the case $\beta = \pi$ [rad] for it corresponds to the anti-phase drive mentioned in the last section (see Fig. 8). The robot moves almost forward at any phase difference β. Although the robot turns a little rightward at $\beta = \pi/2$ [rad], it travels almost straightforward for all choices of β. Thus, it is the traveling speed in the x-direction that varies depending on β. The fastest is the case $\beta = 0$, say *in-phase* drive mode, and the speed tends to be slower as the β increases.

Now let us turn to focus on history of the attitude angle θ. $\theta(t)$ is kept almost constant in the case of $\beta = 0$ (note that $\dot{\theta} = 0$ holds in Eq. (6) for this case). On the other hand, θ starts to oscillate as β gets larger, in particular with larger amplitude A. This partially explains the loss of energy in the forwarding locomotion, as well as the change of traveling speed as depending on β.

5.2 Experiment

We performed physical experiments under the same references and the conditions as the simulation above; compare Fig. 14 for the cases $\beta = 0, \pi/2$ and Fig. 11 for the case $\beta = \pi$.

As shown in these figures, the robot moves almost straightforward in all cases, while the relationship between phase difference and traveling speed shows similar tendency as in the simulation results.

6. CONCLUSION

In this paper, we proposed a mathematical model of the casterboard as an autonomous mobile robot equipped with a pair of mass-beam mechanisms, in the form of nonlinear state equation. We then proposed a control approach for forwarding and turning locomotion that drives the mass-beam actuators so as to track periodic references. Then

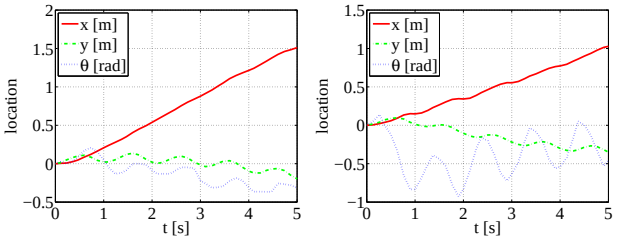

(a) $\beta = 0$ [rad] (b) $\beta = \pi/2$ [rad]

Fig. 14. Robot's location (experiment)

we developed an experimental system of the proposed casterboard robot and realized the forwarding and turning locomotion, to show that the experimental results are well consistent with simulation results. Moreover, we examined the influence on the driving of phase difference of periodic references. In low-frequency range, moving velocity of the robot got higher as the phase difference got smaller, and increased exponentially as the frequency got higher by both simulations and experiments. In the experiments, it was confirmed that a peak of moving velocity appeared in a frequency range, although the peak did not appear in the simulations. Moreover, in the experiments, it was also confirmed that a peak of moving velocity appeared in two frequency ranges, respectively in in-phase drive.

As for physical experiments, we are keen to realize locomotion *without the support casters* by actively balancing the robot's roll angle. We also neglected the dynamics of ψ_i's behavior in response to ϕ_i by assuming their relationship is static. The mathematical model should be refined in the future by taking this dynamics into account.

ACKNOWLEDGEMENT

This research is partially supported by Aihara Project, the FIRST program from JSPS, initiated by CSTP.

REFERENCES

A.M. Bloch. Nonholonomic mechanics and control. *Interdisciplinary Applied Mathematics (IAM)*, 24, 2003.

Y. Kiyasu and M. Ishikawa. Feedback control of nonholonomic mobile robot concerning momentum dynamics: a snakeboard example. *The 3rd IFAC worksop on Lagrangian and Hamiltonian Methods in Nonlinear Control (LHMNLC'06)*, 2006.

K.A. McIsaac and J.P. Ostrowski. A framework for steering dynamic robotic locomotion systems. *The International Journal of Robotics Research*, pages 22:83–97, 2003.

R. M. Murray, S. S. Sastry, and Z. Li. *A Mathematical Introduction to Robotic Manipulation*. CRC Press, 1994.

J. Ostrowski and J. Burdick. he geometric mechanics of undulatory robotic locomotion. *The International Journal of Robotics Research*, pages 17(7):683–701, 1998.

J. Ostrowski, J. Burdick, A.D. Lewis, and R.M. Murray. The mechanics of undulatory locomotion: The mixed kinematic and dynamic case. *International Conference of IEEE Robotics and Automation f95*, pages 1945–1951, 1995.

J. Ostrowski, J.D. Desai, and V. Kumar. Optimal gait selection for nonholonomic locomotion systems. *International Conference of IEEE Robotics and Automationf97*, pages 20–25, 1997.

E. A. Shammas and H. Choset. *Generalized Motion Planning for Underactuated Mechanical Systems*. PhD thesis, Carnegie Mellon University, 2006.